DE GRUYTER Z. Phys. Chem. 2016; aop

Hany M. Abd El-Lateef*, Mohamed Ismael, and
Ahmed H. Tantawy

Empirical and Theoretical Calculations for Corrosion Inhibition of Carbon Steel C1018 in Acidic Solutions Using Some Selected Fatty Acid Surfactants

DOI 10.1515/zpch-2015-0616
Received April 8, 2015; accepted January 23, 2016

Abstract: Three different surfactants based on fatty acids (octanoic, tridecanoic and oleic) and ethylenediamine were synthesized and their chemical structures were confirmed by FT-IR, ^{1}H-NMR and ^{13}C-NMR spectroscopy. The surface-active properties of the prepared surfactants were determined by using interfacial tension.The synthesized surfactants were evaluated as corrosion inhibitors for carbon steel in a solution of 0.50 M HCl at 40 °C. Potentiodynamic polarization, linear polarization resistance corrosion rate and electrochemical impedance spectroscopy measurements were used for this study. Experimental results showed that, the inhibition efficiency increases with increasing the surfactant concentration, getting maximum inhibition efficiency ranged between 97.10 and 99.61% at 400 ppm. Potentiodynamic polarization curves showed that, the three compounds act as mixed type. The adsorption of investigated surfactants obeyed the Langmuir adsorption isotherm, and the thermodynamic parameters were calculated and discussed. Obvious correlation was found between the corrosion inhibition efficiency and the quantum chemical parameters. The obtained theoretical results have been adapted with the experimental data.

Keywords: Impedance Spectroscopy, Corrosion Inhibition, Surfactants, Carbon Steel, Surface Properties, Quantum Chemical Calculations.

***Corresponding author: Hany M. Abd El-Lateef,** Chemistry Department, Faculty of Science, Sohag University, 82524 Sohag, Egypt, e-mail: hany_shubra@yahoo.co.uk
Mohamed Ismael: Chemistry Department, Faculty of Science, Sohag University, 82524 Sohag, Egypt
Ahmed H. Tantawy: Organic Chemistry Department, Faculty of Science, Benha University, Benha, Egypt

1 Introduction

Metallic corrosion causes severe losses to both economy and safety. Thence, many research efforts have been made to prevent or decrease the corrosion of metals in different mediums [1–5]. In several industrial processes hydrochloric acid solution is widely used as an acid wash solution (cleaning, pickling, descaling) for removing rust and scale from mild steel surface [3]. However, when HCl is in contact with metals, it starts to corrode the metallic surfaces. So, in spite of its benefits, it is necessary to find a way for decreasing the corrosion rate caused by the use of HCl. Carbon steel is used in mass amounts in marine applications, chemical processing, petroleum production and refining, construction and metal processing equipment, despite its relatively high cost [4, 5]. Most of these applications have been subjected to acid corrosion in different situations. Therefore, the study of corrosion inhibition of carbon steel in HCl solution is of great importance.

Using of inhibitors is considered as one of the most practical approaches for protecting metals against corrosion, especially in acidic media [6]. Such compounds decrease the corrosion rate by adsorbing into the metal surfaces and blocking their active sites. The adsorption process of surfactants on the electrode surface is influenced by the nature and the surface charge of the metal, the chemical structure of the surfactant, and the nature of the aggressive electrolyte. Organic compounds containing functional electronegative groups such as nitrogen and oxygen are usually good inhibitors since these compounds are easily adsorbed on metal surfaces [6–8].

An important corrosion inhibition tool is the use of surfactant inhibitors. Surfactant inhibitors have many advantages such as low price, easy production, low toxicity and high inhibition efficiency [9–11]. It was reported that the inhibition process by surfactants was attributed primarily to the adsorption of the surfactant molecules, via their functional group, onto the metal surface [12], and so the study the relationship between the adsorption and corrosion inhibition is of great importance. Surfactants have been used for the corrosion inhibition of steel in acidic media [13–15], in chloride saturated solutions [16–19]. It was found that, the adsorption of these surfactants leads to the formation of a single- layer on the surface.

Quantum chemical calculations have been widely used to study reaction mechanisms [20, 21]. They have also been proved to be a very powerful tool for studying inhibition of the corrosion of metals [22, 23]. Recently, the effectiveness of an inhibitor molecule has been related to its spatial as well as electronic structure [24].

The main purpose of this paper is to evaluate the protective ability of oleic acid-ethylenediamine (OEC-**I**), tridecanoic acid-ethylenediamine (TEC-**II**) and Caprylic acid-ethylenediamine (CEC-**III**) surfactants as corrosion inhibitors for carbon steel C1018 in 0.50 M HCl at 40 °C. The acid corrosion-inhibition has been studied using potentiodynamic polarization, electrochemical impedance spectroscopy and linear polarization resistance (LPR) corrosion rate techniques. The surface activity and thermodynamic parameters of micellization and adsorption were studied. The relation between the inhibition efficiency of the investigated compounds and some quantum chemical parameters such as the highest occupied molecular orbital (HOMO) and lowest unoccupied molecular orbital (LUMO) energies, electrophilicity (ω), chemical hardness (η) and dipole moment have been also investigated.

2 Experimental work

2.1 Materials

Fatty acids (Oleic, Tridecanoic and Octanoic (Caprylic)) and ethylenediamine (Assay ≥ 99%) were obtained from SIGMA-ALDRICH Company and were used without further purification.

2.2 Chemical composition of carbon steel alloy C1018

Carbon steel C1018 used for this study has the following composition: C 0.18%, Si 0.24%, Mn 0.50%, P 0.05%, S 0.05%, Ni 0.01%, Cr 0.10% and Fe balance. The mechanical properties of the carbon steel used in this study were given in Abd El-Lateef et al. [18]. The data have been provided by European Corrosion Supplies Ltd.

2.3 Preparation of fatty acid surfactants

Fatty acids (Oleic, Tridecanoic and Octanoic) (0.01 mol) were taken at equimolar ratio with ethylenediamine. The components of reactions were mixed, closed well and placed in a thermostat at temperature ranging between 50–55 °C for a period between 15 and 20 h. Figure 1 shows the chemical name and abbreviation of the used surfactants under study.

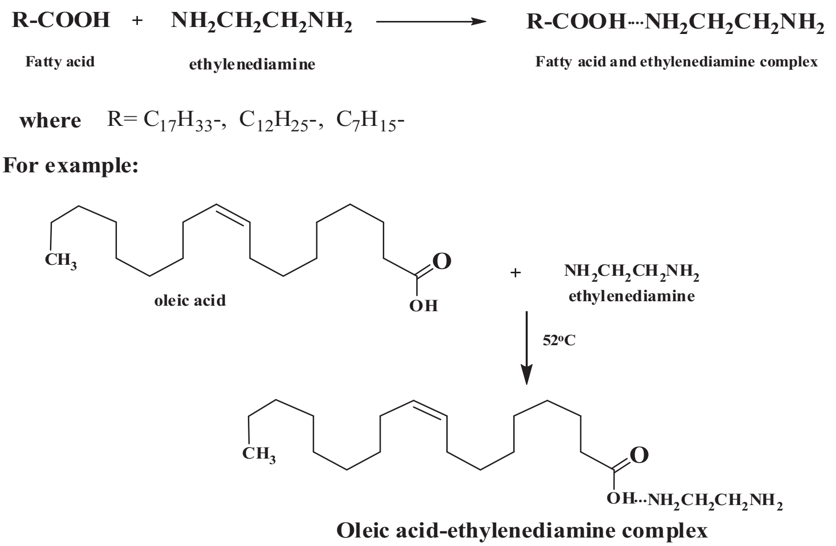

R	Name	Compound and code
$C_{17}H_{33}$-	Oleic acid-ethylenediamine surfactant	OEC-**I**
$C_{12}H_{25}$-	Tridecanoic acid-ethylenediamine surfactant	TEC-**II**
C_7H_{15}-	Octanoic acid-ethylenediamine surfactant	CEC-**III**

Figure 1: Scheme of the synthesis of fatty acids surfactants tested as corrosion inhibitors for carbon steel in 0.5 M HCl.

The chemical structure of the prepared surfactants was identified by physico-chemical (Table 1) and spectroscopic methods. The acid and amine numbers were determined according to procedures as given in Asadov et al. [25]. The electrical conductivity of the prepared surfactants was measured using a conductivity meter, type OK –102/1, made in Hungary. ^1H NMR and ^{13}C-NMR spectra were recorded on a Bruker-TOP SPIN 300.13 MHz and 75.46 MHz spectrometer with chemical shift values (d) in ppm downfield from TMS using $CDCL_3$, acetone-d^6 and CCl_4 as solvents. IR spectra were recorded on a model FT-IR, Spectrum BX spectrometer using KBr disks.

2.4 Test solution

The aggressive solutions were made of Analar grade (BDH) HCl. Appropriate concentration (0.50 M) of the acid was prepared using deionized water. The surfac-

Table 1: Some physico-chemical characteristics of the fatty acid surfactants.

Inhibitors code	External view of the surfactant	Amine number (mg HCl/g)	Solubility of the surfactants	Specific electrical conductivity of 0.5 wt % aqueous solution (ohm^{-1} m^{-1})
OEC-**I**	Muddy-brown viscous liquid	5.10	Readily soluble in water, ethyl alcohol, toluene, CCl_4 and kerosene.	0.001870
TEC-**II**	Viscous liquid of yellow color	3.21	Readily soluble in water, ethyl alcohol, toluene, CCl_4 and kerosene.	0.002050
CEC-**III**	Very viscous of yellow color	2.55	Readily soluble in water, ethyl alcohol, toluene, CCl_4 and kerosene.	0.000124

tant inhibitors were added to the acid aqueous solution in ppm (in terms of w/v) concentration to test the inhibition effect of these compounds on carbon steel.

2.5 Corrosion measurements

The measurements were performed in a one liter glass cell. It consists of typical three electrodes configuration, where the rotating disk carbon steel was used as a working electrode ($A = 4.55$ cm^2). This electrode was used once. Saturated calomel electrode (SCE) was used as a reference and platinum plate as a counter electrode. The cell was filled with the prepared 0.50 M HCl solution. Then this cell was thermostated at 40 °C for 1 h before beginning the experiment. To get rid of any oxide film on the surface, the working electrode was held at −1500 mV for 10 min before measurement. VersaSTAT4 potentiostat/galvanostat and ACM Gill AC instruments connected with laptop were used for the measurements.

2.5.1 Polarization measurements

The working electrode was immersed in the HCl solution for 30 minute until the open circuit potential ($E_{\text{o.c.p}}$) reached. After that, the steel electrode was polarized in both cathodic and anodic directions. The potential increased with a scan rate of 1 mV s^{-1} started from −250 to +250 mV with respect to $E_{\text{o.c.p}}$.

2.5.2 Linear polarization resistance (LPR) corrosion rate

LPR corrosion rate bubble-test is involved to assess the corrosion of carbon steel in 0.50 M hydrochloric acid solution at 40 °C. The LPR corrosion rate measurements were carried out using a laboratory potentiostat (ACM, ACM Instruments, UK). In this method, the working electrode was immersed in the test solution for 1 h until the potential becomes stable. After that, the corrosion rate was measured vs. time for a period 20 h. Data were collected and analyzed using Core Running software (Version 5.1.3.), developed by corrosion monitoring instrumentation [19].

2.5.3 Electrochemical impedance spectroscopy (EIS)

EIS measurements were performed with a phase-sensitive detector (amplifier) (Model 5208) driven by using VersaSTAT4 potentiostat/galvanostat with a frequency response analyzer (FRA) contained in a single unit and connected with laptop. EIS measurements were performed in 0.5 M HCl at 40 °C and in the frequency range from 100 kHz to 0.5 Hz. The amplitude of the voltage perturbation was 10 mV RMS. All experiments were performed at open circuit potential ($E_{\mathrm{o.c.p}}$).

2.6 Surface activity measurements

Measurements of the interfacial tension were carried out using freshly aqueous solutions of the prepared surfactants. The interfacial tension as a function of surfactant concentrations was measured using a drop volume stalagmometer at 20 °C. Interfacial tension values of the three measurements averaged and reported within an accuracy of 0.3 mN/m.

2.7 Computational methods

Geometry optimizations of surfactants were performed using density functional theory (DFT) calculations. All calculations were performed using B3LYP functional and employing 6-311G (d, p) basis set [26]. Gaussian 03 program package was used for all calculations [27]. The quantum chemical indices such as; energy of the highest occupied molecular orbital (E_{HOMO}), energy of the lowest unoccupied molecular orbital (E_{LUMO}), energy band gap $\Delta E = E_{\mathrm{HOMO}} - E_{\mathrm{LUMO}}$, the dipole moment (D. M.), electrophilicity (ω) and chemical hardness (η) were considered.

3 Results and discussion

3.1 Chemical composition of the synthesized fatty acid surfactants

3.1.1 Spectroscopic methods – FTIR, ^{13}C and ^{1}HNMR data

The chemical structure of oleic acid- ethylenediamine surfactant was identified by FT-IR spectroscopy. IR spectra shows an absorption band at the 1574 cm^{-1} characteristic for δ COO^- stretches, in addition to 2847 cm^{-1} for aliphatic C–H, 3103.89 cm^{-1} for NH (amine groups). The FT-IR spectrum showed that, the broad –OH band of the fatty acid was disappeared, confirming that, the proton of acid was transferred to nitrogen atom of amine and formed $-^{+}NH_3$ group. This proves the formation of the target compound.

The results of ^{1}H-NMR and ^{13}C-NMR for oleic acid- ethylenediamine surfactant were found as follow;

^{1}H-NMR (300.13 MHz, $CDCL_3$), δ (ppm): 1.0 (t, 3H, $\mathbf{C\underline{H}_3}-CH_2$), 1.4–1.5 (m, 26H, $\mathbf{C\underline{H}_2}$ chain), 1.51 (t, 2H, $\mathbf{C\underline{H}_2}COO$), 5.4–5.6 (m, 2H,$\mathbf{C\underline{H}=C\underline{H}}$), 2.5–2.7 (m, 4H, $\mathbf{C\underline{H}_2C\underline{H}_2}NH$), 3.53 (s, 1H, $\mathbf{\underline{H}}...NH_2$), 5.31 (s, 2H, $(CH_2)_2\mathbf{N\underline{H}_2}...H$), 2.34 (t, 1H, $CH_2\mathbf{NH_2}$) (Figure S1a in the supplementary file).

^{13}C-NMR (75.46 MHz, $CDCL_3$) δ (ppm): 14.1 ($\mathbf{CH_3}-CH_2$), 20–34 (saturated alkyl chain **14** $\mathbf{CH_2}$), 180 (**COO**), 38 ($NH_2\mathbf{CH_2CH_2}NH_2$), 130–132 ($\mathbf{CH{=}CH}$) (Figure S1b in the supplementary file).

3.1.2 Physico-chemical methods

The physico-chemical properties such as electro-conductivity, amine numbers and solubility in different solvents (water, ethyl alcohol, carbon tetrachloride, toluene and kerosene) of the prepared surfactants were studied. From Table 1, it is noticed that the obtained fatty acid surfactants are generally viscous fluids and their colors vary from light-yellow to yellowish-brown. Measurements of the electrical conductivity of the studied surfactants in aqueous solutions (0.5%) indicated their polarity. Measurements of the amine numbers for all surfactants were done. The data showed that, the amine number increases in the following order:

$$\text{OEC-}\mathbf{I} > \text{TEC-}\mathbf{II} > \text{CEC-}\mathbf{III}$$

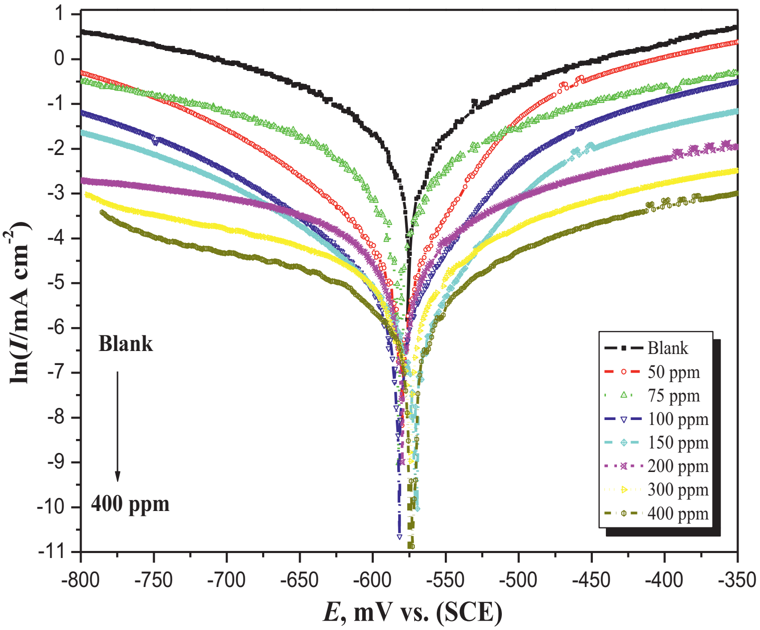

Figure 2: Polarization curves (E–ln I relationship) of carbon steel in 0.50 M HCl containing different concentrations of the OEC-**I** inhibitor at 40 °C.

3.2 Potentiodynamic polarization measurements

Figure 2 shows the cathodic and anodic polarization curves of carbon steel in 0.50 M HCl solution in the absence and presence of different concentrations of the oleic acid-ethylenediamine surfactant (OEC-**I**; as example) at 40 °C. Similar curves were obtained for the other surfactant inhibitors TEC-**II** and CEC-**III** (not shown). The dependence of the degree of surface coverage (θ) and the inhibition efficiency (η %) on the concentration of the inhibitor were calculated using the following equation [28]:

$$\eta\% = 1 - \frac{I_{\text{inh.}}}{I_{\text{uninh.}}} \times 100 \tag{1}$$

$$\theta = \frac{I_{\text{uninh.}} - I_{\text{inh.}}}{I_{\text{uninh.}}} \tag{2}$$

where $I_{\text{uninh.}}$ and $I_{\text{inh.}}$ are the uninhibited and inhibited corrosion current density, respectively. Corrosion rates (CR) was calculated from the polarization measurements using the following equation [29]:

$$\mathrm{CR} = \frac{I_{\mathrm{corr}} \times t \times M}{F \times S \times d} \times 10 \tag{3}$$

where t, M, F, S and d are time (s), the equivalent molar weight of iron (g mol^{-1}), Faraday constant (96 500 C mol^{-1}), the surface area of electrode and density of iron, respectively. The constant 10 is used to convert the unit cm to mm.

It can be clearly seen from Figure 2 that, the addition of OEC-**I** surfactant to the corrosive solution both reduces the anodic dissolution of carbon steel and also retarded the cathodic hydrogen evolution reaction. The corrosion current density as well as corrosion rate of steel considerably reduced in the presence of the investigated inhibitors. These results are indicative for the adsorption of inhibitor molecules on the carbon steel surface [30]. The inhibition of both anodic and cathodic reactions was more and more pronounced with increasing of the inhibitor concentration.

The following electrochemical parameters; cathodic (β_{c}) and anodic (β_{a}) Tafel slopes (calculated by using CoreRunning program), corrosion potential (E_{corr}.), corrosion current density ($I_{\mathrm{corr.}}$), corrosion rates (CR), degree of surface coverage (θ) and the percentage inhibition efficiency (η%) were calculated and listed in Table 2. It is clearly observed that, the corrosion rates (CR) and the corrosion current density (I_{corr}) decreases by increasing the inhibitor doses. This can be attributed to the continuous accumulation of surfactant molecules on the carbon steel surface, which leads to the increase of protective layer thickness and consequently the protection efficiency. While the inhibition efficiency values increase with the increasing of the inhibitor concentration, and the maximum is up to 97.84% at 400 ppm of OEC-**I**. The change in E_{corr} values was observed with the addition of the surfactants. According to Riggs [31], if the displacement in E_{corr} is >85 mV with respect to E_{corr}, the inhibitor can be classified as it is a cathodic or anodic type. In this investigation, the E_{corr} values of all prepared surfactants were shifted slightly toward both anodic and cathodic directions and did not show any definite trend in HCl solutions and the maximum displacement was ±6 mV, which indicated that the surfactants acts as a mixed type inhibitors.

The β_{c} and β_{a} values are approximately constant and independent on the inhibitor concentration. Consequently, the adsorbed inhibitor can be acted by simple blocking the active sites for both anodic and cathodic processes. In other words, the inhibitor decreases the surface area for corrosion without affecting the corrosion mechanism of carbon steel in HCl solution, and only caused inactivation of a part of the surface with respect to the corrosive medium [32].

The decrease in corrosion current densities (I_{corr}), increased in the inhibition efficiency (η%) and the increase in the degree of surface coverage (θ) with increas-

Table 2: Electrochemical parameters and inhibition efficiencies derived from the polarization curves for carbon steel in 0.50 M HCl as function of inhibitor concentration at 40 °C.

Inhibitors code	Conc. of inhibitor (ppm)	I_{corr} (μA cm^{-2})	$-E_{corr}$ (mV (SCEl))	β_a (mV dec^{-1})	$-\beta_c$ (mV dec^{-1})	CR (mm/ year)	θ	η%
Blank	**0.0**	**368**	**577**	**52**	**112**	**5.45**	–	–
OEC-**I**	50	63.55	578	51	110	0.94	0.827	82.73
	75	51.44	579	49	111	0.76	0.860	86.02
	100	28.26	579	47	113	0.41	0.923	92.32
	150	18.25	570	46	109	0.27	0.950	95.04
	200	10.70	579	48	107	0.15	0.970	97.09
	300	9.08	575	45	108	0.13	0.975	97.53
	400	7.94	573	48	106	0.11	0.978	97.84
TEC-**II**	50	70.95	576	48	109	1.05	0.807	80.72
	75	61.45	580	50	110	0.90	0.833	83.30
	100	54.09	578	51	107	0.80	0.853	85.30
	150	35.99	573	46	105	0.53	0.902	90.22
	200	26.75	575	47	107	0.39	0.927	92.73
	300	14.31	576	49	108	0.21	0.961	96.11
	400	12.29	571	46	109	0.18	0.966	96.66
CEC-**III**	50	86.40	575	45	106	1.27	0.765	76.52
	75	72.60	581	46	107	1.07	0.802	80.27
	100	59.94	579	50	111	0.88	0.837	83.71
	150	43.53	572	48	110	0.64	0.881	88.17
	200	29.18	578	49	108	0.43	0.920	92.07
	300	17.88	572	45	109	0.26	0.951	95.14
	400	16.26	574	49	113	0.24	0.955	95.58

ing the inhibitor concentrations showed that, the selected fatty acid surfactants are efficient corrosion inhibitors for carbon steel dissolution in 0.50 M HCl solution. The results also indicate for all inhibitor concentrations, the degree of surface coverage (θ) is near the unity. This suggested that, the inhibition is due to the adsorption of inhibitor molecules on the metal surface and blocking the active sites. In addition, the corrosion inhibition ability of the studied compounds at 400 ppm follows the sequence:

$$\text{OEC-}\mathbf{I}\ (\mathbf{97.84\,\%}) > \text{TEC-}\mathbf{II}\ (\mathbf{96.66\,\%}) > \text{CEC-}\mathbf{III}\ (\mathbf{95.58\,\%})$$

The alkyl chain length and the structure of inhibitor play an important role in the inhibition efficiency of the investigated fatty acid surfactants. The geometric length of the hydrophobic chains can be arranged as the follow; (C_7)

Octanoic acid-ethylenediamine surfactant (CEC-**III**) < (C_{12}) Tridecanoic acid-ethylenediamine surfactant (TEC-**II**) < (C_{17}) Oleic acid-ethylenediamine surfactant (OEC-**I**). By increasing the geometric length, the isolation between metal-medium interaction increased and hence the efficiency of the corrosion inhibitor increased.

3.3 Linear polarization resistance (LPR) corrosion rate

Figure 3a–c shows the change in corrosion rate (CR) with time for carbon steel in 0.50 M HCl solution containing various concentrations of inhibitors OEC-**I**, TEC-**II** and CEC-**III** at 40 °C. After one hour of exposure the inhibitor was added because at this time the corrosion potential got stable, allowing the measurement of the CR before inhibitor injection. The highest corrosion rates in the blank solution were measured to be between 4.01 and 5.58 mm year^{-1}. From Figure 3 it can be observed that, the corrosion rate in the absence of inhibitor tended to increase with time. Increasing of CR in chloride media had been attributed to the galvanic effect between the cementite (Fe_3C) and ferrite phase [33]. Fe_3C is part of the original steel in the non-oxidized state and accumulates on the surface after the preferential dissolution of ferrite (α-Fe) into Fe^{2+}. This in turn leads to an increasing of the corrosion rate over time of exposure [34, 35].

The surface coverage (θ) and the inhibition efficiency ($\eta\%$) values were determined by using the following equations [19]:

$$\eta\% = \frac{\mathrm{CR}_0 - \mathrm{CR}_i}{\mathrm{CR}_0} \times 100 \tag{4}$$

$$\text{Surface coverage} = \theta = 1 - \frac{\mathrm{CR}_i}{\mathrm{CR}_0} \tag{5}$$

where CR_0 and CR_i are the corrosion rate in the absence and presence of inhibitors, respectively. The obtained results of these series of experiments show that, the addition of the surfactants under testing greatly decrease the corrosion rate of carbon steel as the inhibitor dose increases in the given acidic media, giving high levels of $\eta\%$ ranged between 97.10 and 99.61% in the presence of 400 ppm of inhibitors after 20 h of immersion. This means that, these surfactants have a good ability to form protective layers on the metal surface, even in the presence of small concentrations of surfactants. This ability of formation of protective surface layers increased with the increase of surfactant concentration. This ability may be attributed to hydrocarbon chain length in surfactant molecule means a more bulk molecule, which screen the surface from attack and also to the presence of Cl^- ions in the acidic solutions. The adsorption process is facilitated in the presence

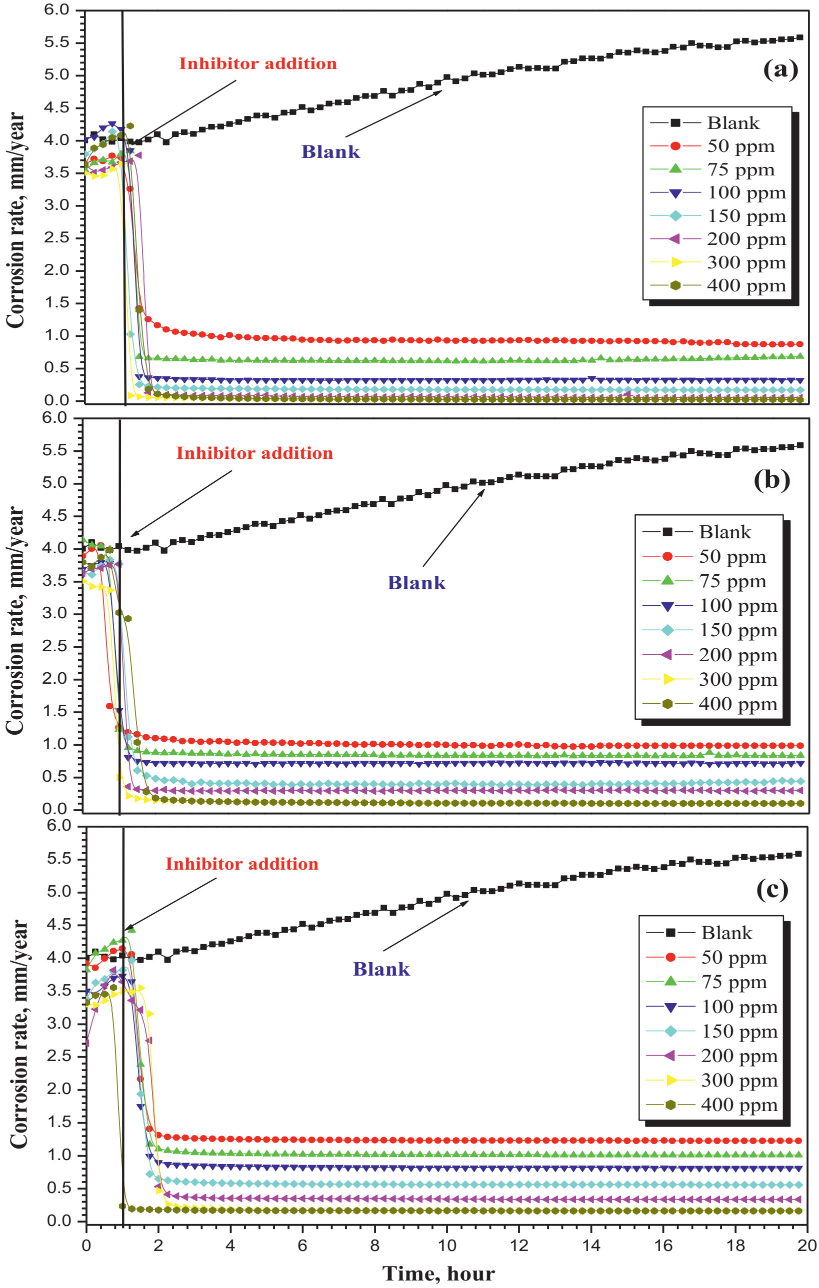

Figure 3: Variation of the Corrosion rate with time for carbon steel in 0.50 M solution of HCl containing different concentrations of inhibitors (a) OEC-**I**, (b) TEC-**II** and (c) CEC-**III** at 40 °C.

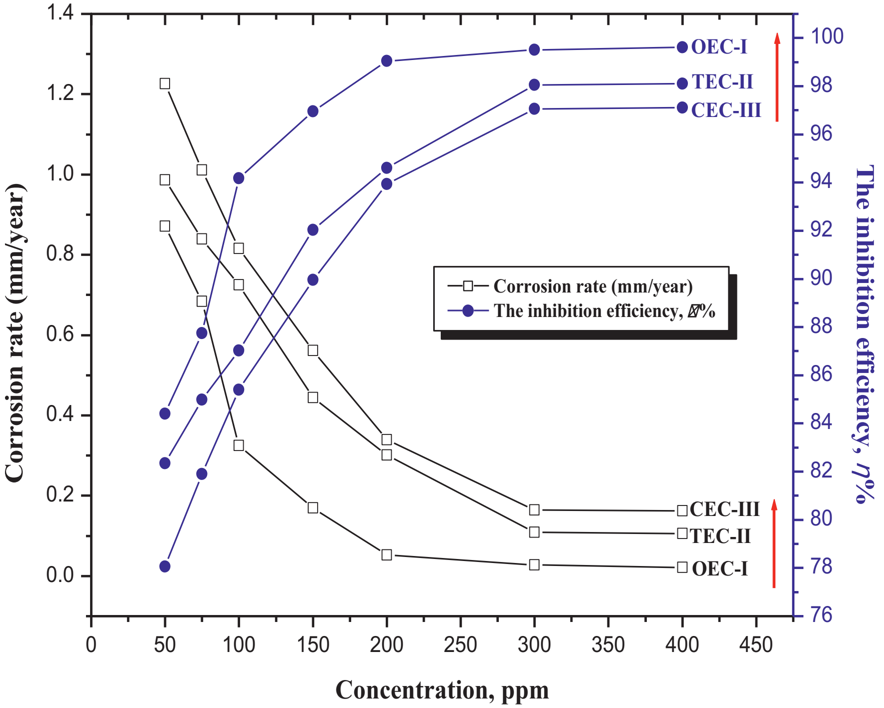

Figure 4: Corrosion rate and Inhibition efficiency of carbon steel immersed in 0.5 M HCl solution with and without different inhibitors at 40 °C. (–□–) Corrosion rate, (–●–) inhibition efficiency.

of Cl^- ions which form intermediate bridges, the negative ends of the halogen dipoles being oriented towards the solution.

Figure 4 shows the calculated values of corrosion rates (CR) and the inhibition efficiencies (η%) in the blank solution (inhibitor free) and those containing various concentrations of the investigated surfactants at 40 °C. The data explained that, the CR and the η% are affected by the inhibitor dose and chemical structure of the inhibitors. The fact that, inhibition efficiencies increase and the corrosion rate (CR) decrease with increasing the inhibitor concentration suggest that the retardant action of the prepared surfactants against metal corrosion, can be interpreted to the adsorption of these inhibitors on the steel surface, retards the dissolution of carbon steel, and the adsorption quantities of surfactants on the investigated substrate increase with concentrations in the aggressive environments [36]. The results also indicated that, the η% values of the compound (OEC-**I**) is greater than that of the other surfactants. The inhibition efficiency of the surfactants decrease in the following order: OEC-**I** > TEC-**II** > CEC-**III**. The highest inhibition efficiency of inhibitor OEC-**I** may be attributed to the increasing of the length of fatty acid chain R from C_7H_{15}- to $C_{17}H_{33}$-.

3.4 Electrochemical impedance spectroscopy (EIS)

EIS measurements of the carbon steel electrode in 0.5 M HCl solution containing different concentrations of inhibitors were performed at 40 °C. Nyquist plots for carbon steel in the investigated acid solution (Figure 5a) showed one depressed capacitive loop. The same trend (one capacitive loop) was also noticed for carbon steel immersed in 0.5 M HCl containing OEC-**I** (50–400 ppm). Similar curves were obtained for the other surfactants. The impedance spectra mainly displayed similar semicircles and the diameter of the semicircles increased with increasing inhibitor concentrations, indicating that, there is no change in the corrosion mechanism [37]. Also, the Bode plots (Figure 5b) refer to the existence of an equivalent circuit that contains a single constant phase element in the steel/acid interface. In the case of EIS measurements, the inhibition efficiency (η%) and double layer capacitance (C_{dl}) can be calculated by the following equations [38, 39]:

$$\eta(\%) = \frac{R_{\mathrm{ct}} - R^0_{\mathrm{ct}}}{R^0_{\mathrm{ct}}} \times 100 \tag{6}$$

$$f\left(-Z^{//}_{\max}\right) = \frac{1}{2\pi C_{\mathrm{dl}} R_{\mathrm{ct}}} \tag{7}$$

where R_{ct} and R^0_{ct} are the charge transfer resistance values with and without inhibitor, respectively. $-Z^{//}_{\max}$ is the maximum imaginary component of the impedance. The semicircular appearance of Nyquist plot shows that, the charge-transfer process takes place during the dissolution of metal [40]. The simplest fitting is represented by Rundles equivalent circuit (inset top Figure 5). In this circuit, R_{s} is the solution resistance, R_{ct} is the charge transfer resistance, and C_{dl} is the double-layer capacitance. This figure reveals a single charge transfer reaction. The impedance diagrams have an approximately semicircular appearance. This indicates that, the corrosion of carbon steel in the HCl solution is controlled by a charge-transfer process.

The main parameters deduced from the analysis of Nyquist and Bode diagrams are given in Table 3. The data show that, by increasing the surfactant concentration, the charge transfer resistance (R_{ct}) increases and the double layer capacitance C_{dl} decreases, indicating that increasing inhibitor concentration decreases the corrosion rate. The decrease in capacitance is caused by reduction in local dielectric constant and/or by increase in the thickness of the electrical double layer. This fact suggests that, the inhibitor molecules can be acted by the ad-

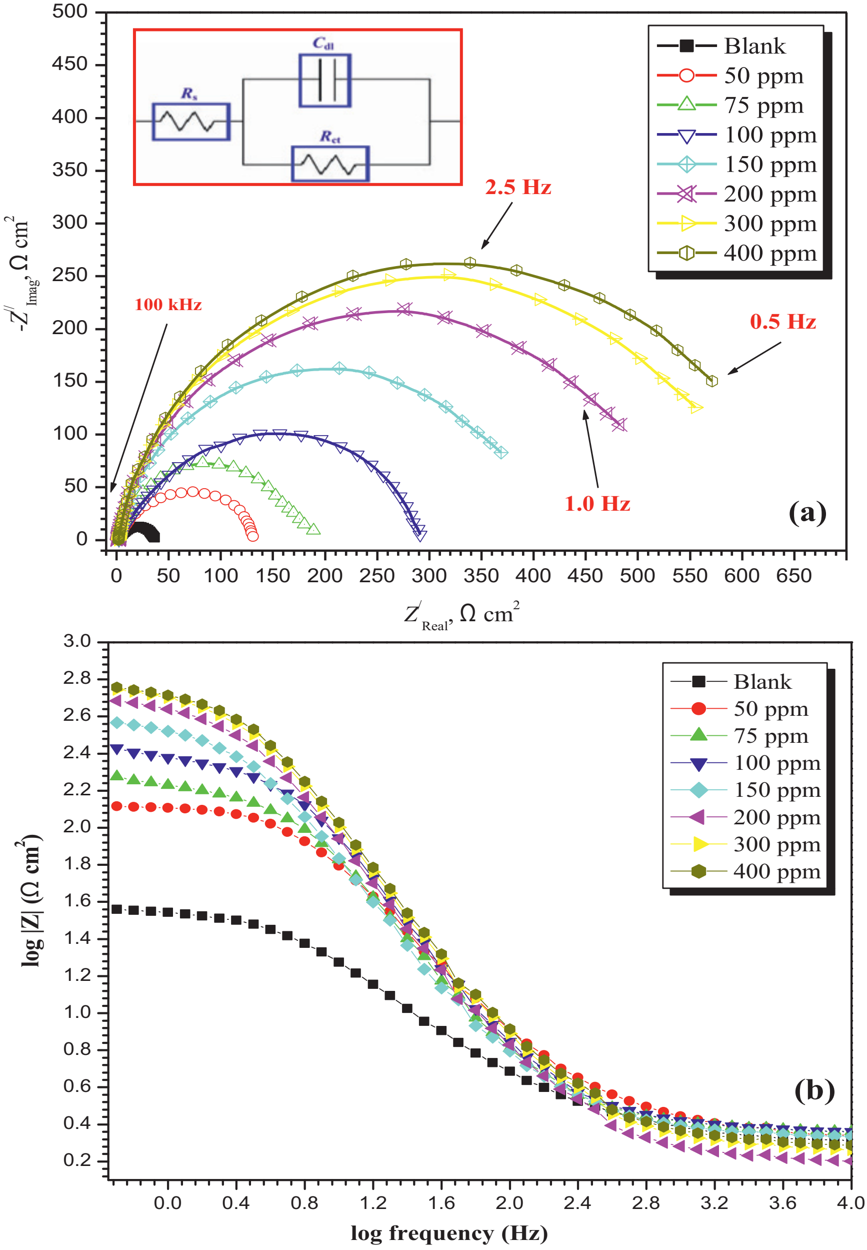

Figure 5: EIS plots for carbon steel in $0.50\ \mathrm{M\ HCl}$ in the absence and presence of different concentration of OEC-I exemplified as: (a) Nyquist and (b) Bode modulus plots. Inset (top) is the equivalent circuit.

Table 3: Impedance electrochemical parameters derived from the Nyquist and Bode plots for carbon steel in 0.50 M HCl solution in the absence and presence of the investigated surfactant inhibitors at 40 °C.

Inhibitors code	Conc. of inhibitor (ppm)	R_s (Ω cm^2)	R_{ct} (Ω cm^2)	$C_{dl} \times 10^{-8}$ (F/cm^2)	The inhibition Efficiency (η%)
Absence	**0.0**	**2.06**	**34**	**46.8**	–
OEC-**I**	50	2.19	137	11.6	75.18
	75	2.29	211	7.5	83.88
	100	2.30	303	5.2	88.77
	150	2.16	456	3.5	92.54
	200	1.59	594	2.6	94.27
	300	1.83	652	2.4	94.78
	400	1.93	688	2.3	95.06
TEC-**II**	50	2.14	132	12.0	74.34
	75	2.24	191	8.3	82.25
	100	2.25	255	6.2	86.70
	150	2.11	344	4.6	90.12
	200	1.55	476	3.3	92.87
	300	1.79	497	3.2	93.16
	400	1.89	532	2.9	93.62
CEC-**III**	50	2.08	127	12.5	73.29
	75	2.17	180	8.8	81.20
	100	2.18	237	6.7	85.65
	150	2.05	311	5.1	89.07
	200	1.51	415	3.8	91.82
	300	1.74	431	3.6	92.11
	400	1.83	457	3.4	92.57

sorption at the metal/solution interface [41]. The diameter of the capacitive loop obtained in HCl solution was increased in the presence of the prepared surfactants indicating an inhibition of the corrosion process.

By comparison between inhibition efficiency values (η%) which are calculated from the three different techniques (potentiodynamic polarization, LPR corrosion rate and EIS), we found that, all have the same trend. In other words, the η% values increase with increasing the inhibitor dose and the maximum η% values are obtained at 400 ppm (95.06, 93.62 and 92.57% for OEC-**I**, TEC-**II** and CEC-**III**, respectively). At the same inhibitor concentrations, the order of increasing η% of the investigated inhibitors is: OEC-**I** > TEC-**II** > CEC-**III**. Because of the following reasons:

- The values of base number for the inhibitors OEC-**I**, TEC-**II** and CEC-**III** were found to be 5.10, 3.21 and 2.55 (tabref1), respectively. From these values, it is clear that the basicity increases in the order: OEC-**I** > TEC-**II** > CEC-**III** and the inhibition efficiency of these surfactants increases in the same order. The increase of base number of surfactants led to increase the proton convergence and charge. Thus by taking suitable substitutions in the inhibitor molecule an improvement in the degree of inhibition of corrosion has been achieved.
- In the literature [19, 36], the inhibition efficiencies values (η%) depend on the molecular size of inhibitors. The η% values of inhibitor OEC-**I** (95.06%) are higher than those of inhibitors TEC-**II** (93.62%) and CEC-**III** (92.57%), due to the larger molecular size of the OEC-**I** compared with those of TEC-**II** and CEC-**III**. The molecular size of the surfactant has a direct effect on its η% values. The increase of hydrocarbon chain of the inhibitor leads to increase of molecular size. The increase of η% is due to the inductive effect of the methyl groups.

3.5 Surface activity measurements

The interfacial tension values for the different surfactant concentrations were determined at 20 °C. The values of interfacial tension were plotted versus the concentrations of surfactant, $\ln C$ (Figure 6). The surface tension-concentration curve of the prepared surfactant solutions showed two characteristic regions (Figure 6). The first is at low concentrations and characterized by continuous decrease of the surface tension values due to the adsorption of the hydrocarbon chains of surfactant molecules at the interface. In the second region, the surface tension variation is almost stable by increasing the concentration. That indicates no further adsorption of surfactant molecules is occurred at the interface [42, 43]. The intercept of the two straight lines designates the critical micelle concentration (CMC). The surface active properties of the prepared surfactants; maximum surface excess ($\Gamma_{\max}$), minimum area per molecule ($A_{\min}$) and effectiveness (π_{cmc}) were calculated using the following equations [44–46]:

$$\Gamma_{\max} = \frac{-1}{nRT}\left(\frac{\mathrm{d}\gamma}{\mathrm{d}\ln C}\right)_T \tag{8}$$

$$A_{\min} = \frac{10^{16}}{\Gamma_{\max}} \times N_A \tag{9}$$

$$\Pi_{\mathrm{cmc}} = \gamma_0 - \gamma_{\mathrm{cmc}} \tag{10}$$

where $\partial\gamma/\partial \ln C$ is the maximum slope (the slope of a plot interfacial tension versus $\ln C$ curves below CMC), γ_0 is the surface tension of pure water, γ_{cmc} is the sur-

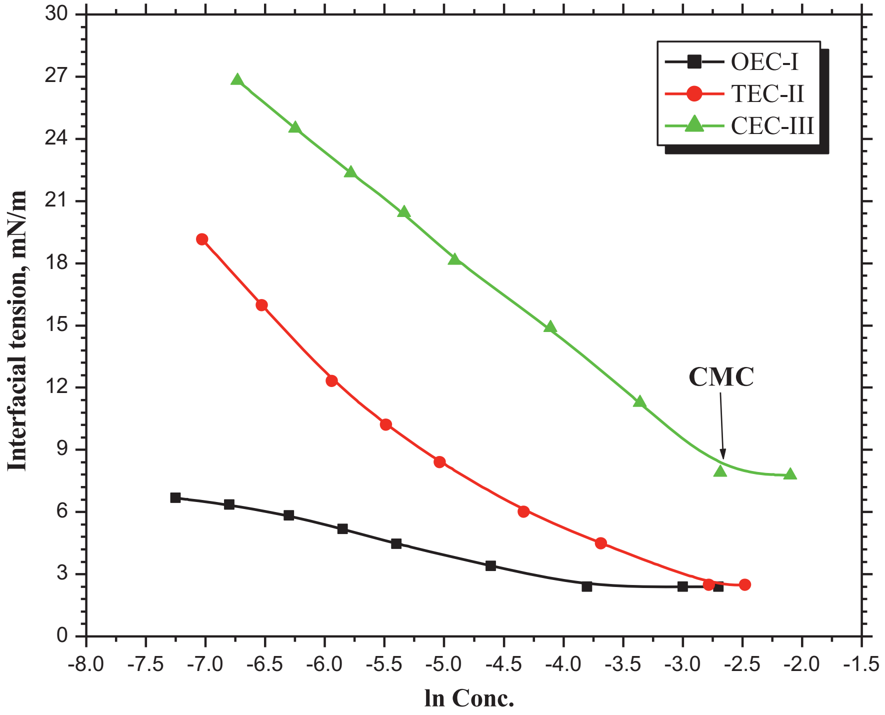

Figure 6: Interfacial tensions versus concentration of fatty acid surfactants in aqueous solution at 20 °C.

face tension at CMC, R is the molar gas constant, N_A is the Avogadro's number, T is the absolute temperature and n is the number of ions that originate in solution by dissociation of the surfactant and whose concentration vary at the surface when changing the bulk solution concentration (assumed as 2 in our calculations). The standard free energy of micellization and adsorption are given by [42]:

$$\Delta G^0_{\text{mic}} = RT \ln \text{CMC} \tag{11}$$

$$\Delta G^0_{\text{ads}} = \Delta G^0_{\text{mic}} - 0.6023\pi_{CMC} A_{\text{min}} \tag{12}$$

The interfacial activity (I_{activ}) is expressed by physico-chemical parameter $\Delta G^0_{\text{ads}}/A_{\text{min}}$. The data obtained from surface tension measurements are summarized in Table 4. The effectiveness (Π_{CMC}) values increased by increasing the hydrophobic chain length from $C_7H_{15^-}$ to $C_{17}H_{33^-}$. From these results it is noted that OEC-**I** compound is the most effective ones.

The data in Table 4 show that, Γ_{max} shifts to lower values by increasing of hydrophobic surfactant length. The reducing of the maximum surface excess values

Table 4: Surface active properties of the synthesized fatty acid surfactants.

Inhibitors code	CMC × 10^{-4} ($\mathrm{mol\,l^{-1}}$)	γ_{CMC} (mN/m)	Π_{CMC} (mN/m)	$\Gamma_{\max} \times 10^{10}$ ($\mathrm{mol\,cm^{-2}}$)	$A_{\min}$ ($\mathrm{nm^2}$)	$\Delta G^0_{\mathrm{mic}}$ (kJ/mol)	$\Delta G^0_{\mathrm{ads}}$ (kJ/mol)	$\Delta G^0_{\mathrm{ads}}/A_{\min}$ ($\mathrm{kJ/mol\,nm^2}$)
OEC-**I**	1.1	2.39	44.11	0.78	2.20	−10.9	−69.34	−31.52
TEC-**II**	7.3	2.48	44.02	1.60	1.04	−6.2	−33.77	−32.47
CEC-**III**	24.5	4.22	42.28	5.40	0.30	−1.3	−8.94	−29.80

indicates a decrease in the molecules adsorbed at the interface, and as a result the area available for each molecule will increase [25].

By inspection of the obtained data (Table 4), it is found that $A_{\min}$ increases by increasing the hydrophobic length in the surfactant molecules. This behavior may be attributed to that the increase of hydrophobic length of investigated surfactants leads to increasing the molecular weight and the availability of the surfactant to be adsorbed on the interface per molecule will decrease. In other words, the larger the molecule occupied larger area per molecule. Thus, there will be a need for a small number of surfactants for the occupation to provide the best active characteristics [25].

From Table 4, it can be seen that, the free energy changes of micellization and adsorption ($\Delta G^0_{\mathrm{ads}}$ and $\Delta G^0_{\mathrm{mic}}$) show negative sign, showing the spontaneity of the two processes at the investigated temperature. Moreover, $\Delta G^0_{\mathrm{ads}}$ increase in negativity than $\Delta G^0_{\mathrm{mic}}$, indicating the tendency of the molecules to be adsorbed at the interface [47]. Also, it shows that $\Delta G^0_{\mathrm{mic}}$ decreases gradually by increasing the alkyl (hydrophobic) chain length.

The data also showed that, the CMC values decrease with increasing in the length of the hydrocarbon chain of the investigated surfactants. It has to be noted that for a surfactant to be an excellent corrosion inhibitor it should exhibit a low CMC value, because the inhibition effectiveness decreases as the CMC value increases. Based on this view, the surfactant OEC-**I** show the lowest CMC value (Table 4) and hence it considered the most effective corrosion inhibitor for carbon steel in HCl solution. This, in fact, agrees with the electrochemical measurements. Surfactant OEC-**I** appears to create a good hydrophobic physical barrier to the aggressive ions and this account for its high inhibition efficiency.

3.6 Adsorption isotherm and thermodynamic calculations

Adsorption isotherms are very important to determine the mechanism of organo-electrochemical reactions [32]. The corrosion process is inhibited by the adsorption of studied surfactants on the metal surface. In order to obtain the type of adsorption isotherm, the experimental data were applied to different adsorption isotherm equations such as the Langmuir, Frumkin, Temkin, Freundlich and Flory-Huggins. By far the best fit was obtained with the Langmuir isotherm. Langmuir adsorption isotherm is described by the following equation [48–51]:

$$\frac{C_{\mathrm{inh}}}{\theta} = C_{\mathrm{inh}} + \frac{1}{K_{\mathrm{ads}}} \tag{13}$$

where C_{inh} is the inhibitor concentration, K_{ads} is the adsorption equilibrium constant and θ is the surface coverage. Figure 7 shows, a plots of $C_{\mathrm{inh.}}/\theta$ vs. C_{inh} at 313 K gives a straight line with excellent correlation coefficients ($R > 0.999$; Figure 7) and slope near to unity (1.03, 1.08 and 1.03 for OEC-**I**, TEC-**II** and CEC-**III**, respectively), confirming the validity of this assumption.

The slope of the straight line (K_{ads}) had been found to be 9.90×10^3, 9.80×10^3 and 9.65×10^3 M^{-1} for OEC-**I**, TEC-**II** and CEC-**III**, respectively, suggesting that the adsorbed inhibitor molecules formed monolayer on the carbon steel surface and there is no interaction among the adsorbed inhibitor molecules [52]. On the other hand, the high values of the adsorption equilibrium constant for the investigated surfactants indicated powerful adsorption on the carbon steel surface in the aggressive media under study. The large values of K_{ads} mean efficient adsorption and thus the efficiency of inhibition is improved [53]. The high values of the obtained K_{ads} for the investigated inhibitors are consistent with the high η%.

The standard free energy of adsorption ($\Delta G^0_{\mathrm{ads}}$) can be given as the following equation [50]:

$$K_{\mathrm{ads}} = \frac{1}{55.5}\exp\left(-\frac{\Delta G^0_{\mathrm{ads}}}{RT}\right) \tag{14}$$

where 55.5 is the concentration of water in the solution in mol l^{-1}, R and T are the universal gas constant and the thermodynamic temperature, respectively [54]. Generally, the values of $\Delta G^0_{\mathrm{ads}}$ up to -20 kJ mol^{-1} are consistent with the electrostatic interaction between the charged molecules and the charged metal (physical adsorption). While those around -40 kJ mol^{-1} or higher are associated with chemisorption as a result of the sharing or transfer of electrons from organic molecules to the metal surface to form a coordinate bond (chemisorption) [55, 56]. In the present study, the values of $\Delta G^0_{\mathrm{ads}}$ were found to be -36.04, -36.01 to -35.97 kJ mol^{-1} for OEC-**I**, TEC-**II** and CEC-**III**, respectively (slightly negative than -20 kJ mol^{-1}); which suggests that the adsorption of surfactant molecules on the electrode surface in 0.5 M of hydrochloric acid solution is not merely physisorption or chemisorption but obeying comprehensive adsorption (Physical and chemical adsorption) [57].

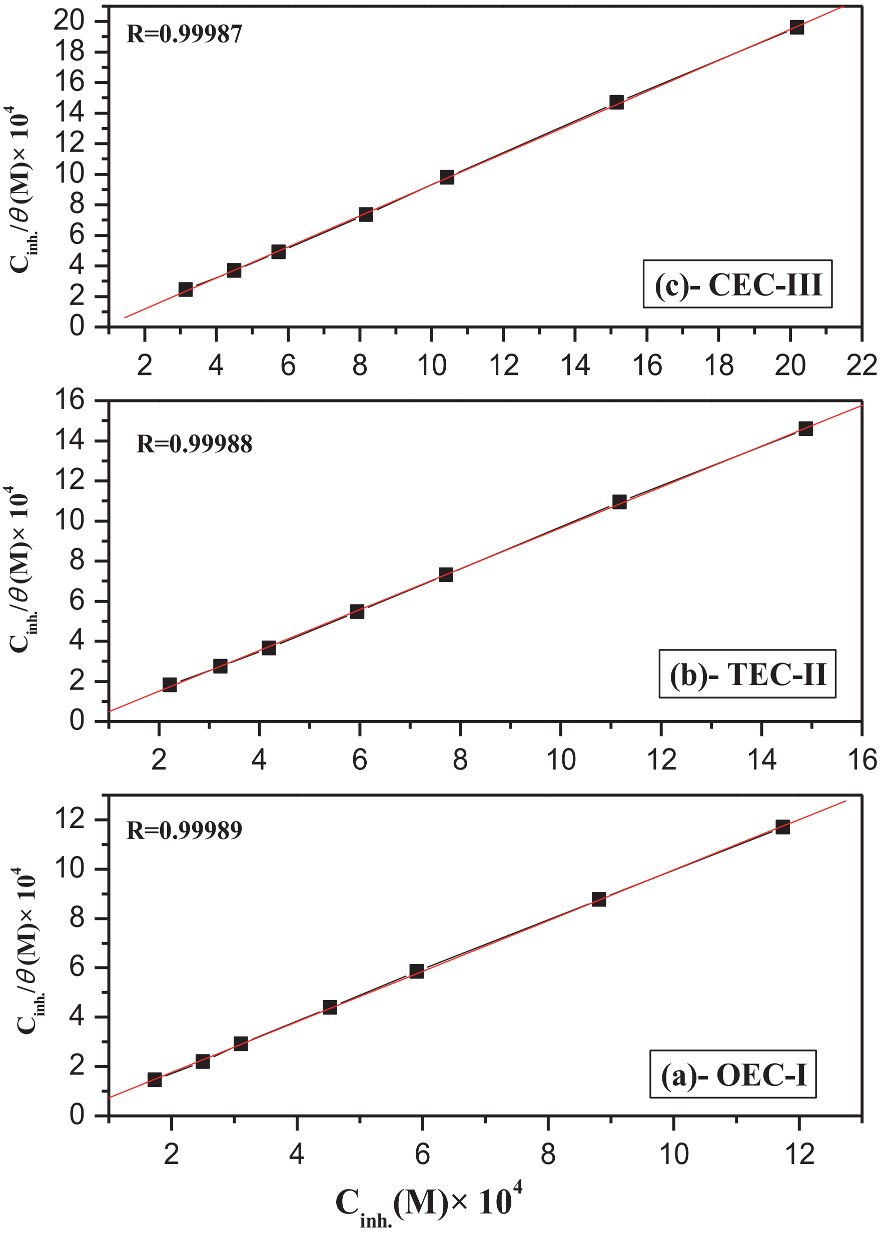

Figure 7: Curve fitting of the corrosion data obtained from potentiodynamic polarization measurements for carbon steel in 0.5 M HCl solution containing various concentrations of inhibitors according to Langmuir adsorption isotherm model at 40 °C.

3.7 Theoretical study

Quantum chemical methods have already proven to be very useful in determining the molecular structure as well as elucidating the electronic structure and reactivity [58]. Quantum chemical calculations were carried out to investigate the relationship between the molecular structures of the surfactants and their inhibition effect. The optimized minimum energy geometrical configurations and the frontier molecule orbital density distributions of the molecules are shown in Figure 8. Geometric structures and electronic properties of studied inhibitors were calculated by Gaussian 03 package with 6-311G (d,p) basis set.

Table 5 shows the values of some quantum chemical parameters, namely the energy of HOMO (E_{HOMO}), energy of LUMO (E_{LUMO}), the energy gap ($\Delta E = E_{\mathrm{LUMO}} - E_{\mathrm{HOMO}}$), chemical hardness ($\eta$), electronic chemical potential (μ) and electrophilicity (ω) for the surfactants models. From this table, one can order the activity as OEC-**I** > TEC-**II** > CEC-**III**. This order was based on the obtained chemical hardness η and electronic chemical potential μ. However the insignificant difference between η and μ values makes it not conclusive and reflects the similarities on their reactivity.

Figure 8 shows the optimized structures of the investigated surfactants, where it can be observed that the amino group of ethylenediamine was oriented towards the carboxylic group of the fatty acid. The chemical behavior of the models might be investigated from their electronic configurations, specifically from the HOMO and LUMO [59]. High value of E_{HOMO} for the investigated models is likely to a tendency of the molecule to donate electrons to appropriate acceptor molecule of low empty molecular orbital energy and indicates also the better inhibition efficiency. On the other hand, the lower E_{LUMO}, are more probable to accept electrons.

It has been reported in the literature that, the higher the E_{HOMO} energy of the inhibitor, the greater trend of offering electrons to unoccupied d orbital of the investigated metal, and hence the higher the corrosion inhibition efficiency. In addition, the lower values of E_{LUMO} are stronger the electron accepting abilities of the molecules, as the LUMO-HOMO energy gap decreases, the efficiency of inhibitor increases [60]. In this work, the calculations showed that the calculated HOMO energies for OEC-**I**, TEC-**II** and CEC-**III** are −6.49, −6.51 and −6.52 eV, respectively; (Figure 8). It is clear that the lower HOMO corresponds to CEC-**III** (−6.52 eV) which exhibited the lower inhibition efficiency and the highest value is obtained by OEC-**I** (−6.49 eV) which is the best one. The calculated E_{LUMO} values are 0.55, 56 and 0.57 eV for OEC-**I**, TEC-**II** and CEC-**III**, respectively (Figure 8). This can explain that the highest inhibition efficiency of OEC-**I** surfactant is due to the increasing its HOMO and decreasing its LUMO energies.

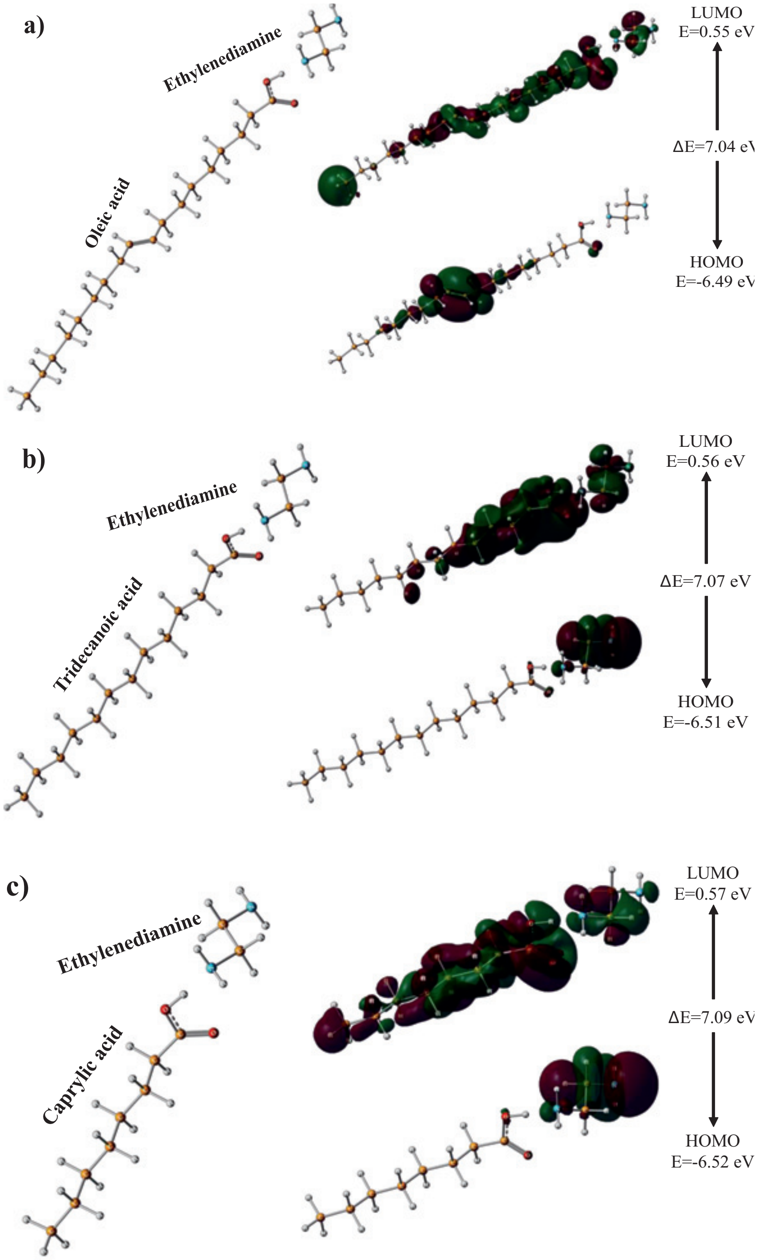

Figure 8: Optimized structures and frontier molecular orbitals of a) Oleic acid-ethylenediamine (OEC-**I**), b) Tridecanoic acid-ethylenediamine (TEC-**II**) and c) Octanoic (Caprylic) acid-ethylenediamine (CEC-**III**) surfactants.

Table 5: Quantum chemical parameters of the surfactants models.

Models	D. M. (Debye)	E_{HOMO} (eV)	E_{LUMO} (eV)	ΔE (eV)	η (eV)	μ (eV)	ω (eV)	η%
OEC-**I**	1.68	−6.49	0.55	7.04	3.54	−2.99	1.25	99.61
TEC-**II**	1.62	−6.51	0.56	7.07	3.53	−2.98	1.26	98.10
CEC-**III**	1.61	−6.52	0.57	7.09	3.52	−2.97	1.27	97.10

E_{HOMO}: Energy of the highest occupied molecular orbital.
E_{LUMO}: Energy of the lowest unoccupied molecular orbital.
ΔE: Energy gap between LUMO and HOMO.
η: Chemical hardness.
μ: Electronic chemical potential.
ω: Electrophilicity.
η%: Inhibition efficiency from LPR corrosion rate measurements.

The energy gap, $\Delta E = (E_{\text{LUMO}} - E_{\text{HOMO}})$, is an important parameter as a function of reactivity of the inhibitor molecule towards the adsorption on metallic surface [61, 62]. As the energy gap (ΔE) decreases, the efficiency of the inhibitors is improved. Data in Table 5 show that, the percent of inhibition efficiency is increased with decreasing ΔE. This is in a good agreement with the experimental observations suggesting that, the OEC-**I** inhibitor has the highest inhibition efficiency among the investigated inhibitors. Electrophilicity index (ω) has been defined by Parr et al [63] as in Equation (15):

$$\omega = \frac{\mu^2}{2\eta} \tag{15}$$

where μ is the chemical potential takes the average value, i.e, $\mu \approx -(I + A)/2$ where I is the ionization potential of the donor and A is the electron affinity of the acceptor, η is the chemical hardness, i.e., $\eta \approx (I - A)/2$. Generally, the electrophiles are electron deficient and hence favor to accept electrons and form bonds with nucleophiles. Thus electrophilicity is a useful structural depictor of reactivity and is considerably used in the analysis of the chemical reactivity of molecule [64]. The molecule with low potential is a good electrophile; an extremely hard molecule has weak electron acceptability. Consequently, a measure of molecular electrophilicity depends on both the chemical potential and the chemical hardness. From Table 5, it is clear that, the lower electrophilicity (ω; 1.25 eV) and highest chemical hardness (η; 3.54 eV) was found corresponds to OEC-**I** inhibitor, this could lead to the conclusion that, the highest protection is formed in the presence of OEC-**I**.

The data in Table 5 show that, the value of dipole moment (**D. M.**) for OEC-**I** model is higher compared with those of other inhibitors. The increase of the dipole moment can lead to increase of inhibition, which could be related to the dipole–dipole interaction of molecules and metal surface [65]. Finally, according to a series of properties calculated for each molecule shown in Table 5 the reactivity order, that is, the inhibitive effectiveness order for the molecules are: OEC-**I** > TEC-**II** > CEC-**III**. The calculated results are in agreement with experimental results.

4 Conclusion

A systematic study of the corrosion inhibition of carbon steel in 0.50 M HCl in the presence of three fatty acid surfactants by electrochemical and quantum chemical calculations led to the following conclusion:

1. All studied surfactants showed good inhibition properties for the corrosion of carbon steel in 0.50 M HCl. The inhibition efficiency increased with increasing the inhibitor concentrations as well as the hydrophilic chain length, getting maximum inhibition efficiency ranged between 97.10 and 99.61% at 400 ppm.
2. Evaluation of potentiodynamic polarization measurements revealed that the studied three fatty acid surfactants behave as mixed type inhibitors.
3. The corrosion process was inhibited by the adsorption of studied surfactants on the metal surface. Adsorption process obeyed Langmuir adsorption isotherm.
4. The values of $\Delta G^0_{\mathrm{ads}}$ showed that the studied inhibitors have mixed mode of adsorption (Physical and chemical adsorption).
5. The CMC values showed a decrease in CMC with increasing in the length of the hydrocarbon chain of the investigated fatty acid surfactants.
6. Thermodynamic parameters of micellization (ΔG^0_{mic}) and adsorption ($\Delta G^0_{\mathrm{ads}}$) provide a further confirmation that the selected surfactants predominance of the adsorption than the micellization.
7. A good correlation was found in between the quantum chemical parameters (E_{HOMO}, E_{LUMO}, energy gap (ΔE), electrophilicity (ω), chemical hardness (η)) and experimentally obtained inhibition efficiencies of the studied surfactant inhibitors.

Acknowledgement: The authors would like to thank Professor V. M. Abbasov – Director of Institute of Petrochemical Processes – Azerbaijan National Academy of Sciences for his help in LPR corrosion rate test. Special thanks for the IT unite at

Sohag university for providing access to the server for performing the theoretical calculations.

References

1. H. M. Abd El-Lateef, Corros. Sci. **92** (2015) 104.
2. H. M Abd El-Lateef, M. Ismael, and I. Mohamed, Corros Rev. **33** (2015) 77.
3. H. M Abd El-Lateef, A. M Abu-Dief, L. H. Abdel-Rahman, E. C. Sañudo, and N. Aliaga-Alcalde, J. Electroanal. Chem. **743** (2015) 120.
4. S. T. Zhang, Z. H. Tao, W. H. Li, and B. R. Hou, Appl. Surf. Sci. **255** (2009) 6757.
5. B. Mernari, H. El Attari, M. Traisnel, F. Bentiss, and M. Lagrenee, Corros. Sci. **40** (1988) 391.
6. H. Ju, Z. P. Kai, and Y. Li, Corros. Sci. **50** (2008) 865.
7. I. Ahamad, R. Prasad, and M. A. Quraishi, Corros. Sci. **52** (2010) 933.
8. L. Herrag, B. Hammouti, S. Elkadiri, A. Aouniti, C. Jama, H. Vezin, and F. Bentiss, Corros. Sci. **52** (2010) 3042.
9. M. M. Caroline, P. Christian, C. S. Hannes, K. Boris, and A. A. Ilhan, Langmuir, **24** (2008) 14269.
10. A. Kumar, E-J. Chem. **5** (2008) 275.
11. M. El Azhar, B. Mernari, M. Traisnel, F. Bentiss, and M. Lagrenee, Corros. Sci. **43** (2001) 2217.
12. N. A. Negm, A. M. Al Sabagh, M. A. Migahed, H. M. Abdel Bary, and H. M. El Din, Corros. Sci. **52** (2010) 2122.
13. Q. Zhang, Z. Gao, F. Xu, and X. Zou, Colloid. Surface. A **380** (2011) 191.
14. M. A. Migahed, E. M. S. Azzam, and A. M. Al Sabagh, Mater. Chem. Phys. **85** (2004) 273.
15. A. Döner, R. Solmaz, M. Özcan, and G. Kardas, Corros. Sci. **53** (2011) 2902.
16. H. M. Abd El-Lateef, V. M. Abbasov, L. I. Aliyeva, E. E. Qasimov, and I. T. Ismayilov, Mater. Chem. Phys. **142** (2013) 502.
17. H. M. Abd El-Lateef, V. M. Abbasov, L. I. Aliyeva, and E. E. Qasimov, J. Korean Chem. Soc. **57** (2013) 25.
18. H. M. Abd El-Lateef, V. M. Abbasov, L. I. Aliyeva, E. E. Qasimov, E. N. Efremenko, T. A. Ismayilov, S. A. Mamedxanova, and I. T. Ismayilov, Int. J. Thin Film. Sci. Tec. **2** (2013) 91.
19. I. T. Ismayilov, H. M. Abd El-Lateef, V. M. Abbasov, E. N. Efremenko, L. I. Aliyeva, and C. K. Salmanova, Int. J Corros. Scale. Inhib. **4** (2015) 57.
20. M. K. Awada, M. S. Metwally, S. A. Soliman, A. A. El-Zomrawy, and M. A. Bedair, J. Ind. Eng. Chem. **20** (2014) 796.
21. K. C. Emregul and M. Hayvali, Corros. Sci. **48** (2006) 797.
22. K. F. Khaled, K. B. Samardžija, and N. Hackerman, Electrochim. Acta **50** (2005) 2515.
23. S. Xia, M. Qiu, L. Yu, F. Liu, and H. Zhao, Corros. Sci. **50** (2008) 2021.
24. F. Bentiss, M. Lebrini, M. Lagrenée, M. Traisnel, A. Elfarouk, and H. Vezin, Electrochim. Acta **52** (2007) 6865.
25. Z. H. Asadov, A. H. Tantawy, I. A. Zarbaliyeva, and R. A. Rahimov, Egypt. J. Pet. **22** (2013) 261.
26. P. J. Hay and W. R. Wadt, J. Chem. Phys. **82** (1985) 270.

27. M. J. Frisch, G. W. Trucks, H. B. Schlegel, G. E. Scuseria, M. A. Robb, J. R. Cheeseman, J. A. Montgomery, T. Vreven, K. N. Kudin, J. C. Burant, J. M. Millam, S. S. Iyengar, J. Tomasi, Barone Vo, B. Mennucci, M. Cossi, G. Scalmani, N. Rega, G. A. Petersson, H. Nakatsuji, M. Hada, M. Ehara, K. Toyota, R. Fukuda, J. Hasegawa, M. Ishida, T. Nakajima, Y. Honda, O. Kitao, H. Nakai, M. Klene, X. Li, J. E. Knox, H. P. Hratchian, J. B. Cross, V. Bakken, C. Adamo, J. Jaramillo, R. Gomperts, R. E. Stratmann, O. Yazyev, A. J. Austin, R. Cammi, C. Pomelli, J. W. Ochterski, P. Y. Ayala, K. Morokuma, G. A. Voth, P. Salvador, J. J. Dannenberg, V. G. Zakrzewski, S. Dapprich, A. D. Daniels, M. C. Strain, O. Farkas, D. K. Malick, A. D. Rabuck, K. Raghavachari, J. B. Foresman, J. V. Ortiz, Q. Cui, A. G. Baboul, S. Clifford, J. Cioslowski, B. B. Stefanov, G. Liu, A. Liashenko, P. Piskorz, I. Komaromi, R. L. Martin, D. J. Fox, T. Keith, M. A. Al-Laham, C. Y. Peng, A. Nanayakkara, M. Challacombe, P. M. W. Gill, B. Johnson, W. Chen, M. W. Wong, C. Gonzalez, and J. A. Pople, Gaussian 03, Revision C. 01, Gaussian, Inc., Wallingford, CT (2004).
28. A. El-Sayed, H. S. Mohran, and H. M. Abd El-Lateef, Corros. Sci. **52** (2010) 1976.
29. H. M. Abd El-Lateef, Res. Chem. Intermed., (2015) DOI:10.1007/s11164-015-2207-y.
30. A. El-Sayed, H. S. Mohran, and H. M. Abd El-Lateef, Monatsh. Chem. **7** (2011) 558.
31. O. L. Riggs, Corrosion **31** (1975) 128.
32. M. A. Amin, J. Appl. Electrochem. **36** (2006) 215.
33. N. Staicopolus, J. Electrochem. Soc. **110** (1963) 1121.
34. J. Crolet, N. Thevenot, and S. Nesic, Corrosion **54** (1998) 194.
35. H. M. Abd El-Lateef, V. M. Abbasov, L. I. Aliyeva, and M. M. Khalaf, Egypt. J. Pet. **24** (2015) 175.
36. A. El-Sayed, H. S. Mohran, and H. M. Abd El-Lateef, Corros. Sci. **52** (2010) 72.
37. F. M. Reis, H. G. de Melo, and I. Costa, Electrochim. Acta **51** (2006) 1780.
38. G. E. Badr, Corros. Sci. **51** (2009) 2529.
39. I. Ahamad and M. A. Quraishi, Corros. Sci. **51** (2009) 2006.
40. S. Muralidharan, S. Syed Azim, L. John Berchmans, and S. V. K. Iyer, Anti-Corros. Method. Mater. **44** (1997) 30.
41. H. A. Sorkhabi, B. Shaabani, and D. Seifzadeh, Electrochim. Acta **50** (2005) 3446.
42. M. J. Rosen, *Surfactants and Interfacial Phenomena*, 2nd edn., Wiley, New York (1992).
43. N. A. Negm, N. G. Kandile, I. A. Aiad, and M. A. Mohammad, New eco-friendly cationic surfactants: Synthesis, characterization and applicability as corrosion inhibitors for carbon steel in $1\ \mathrm{N\ HCl}$, Colloid. Surface. A **391** (2011) 224.
44. A. M. Al-Sabagh, N. M. Nasser, M. A. Migahed, and N. G. Kandil, Egypt. J. Pet. **20** (2011) 59.
45. T. Takeshita, T. Shimohara, and S. Maeda, J. Am. Oil Chem. Soc. **59** (1982) 104.
46. N. A. Negm, A. F. M. El-Farargy, E. A. Abdel Halim, S. El-lboudy, and A. I. Ahmed, J. Surfact. Deterg. **17** (2014) 1203.
47. A. M. Badawi, M. A. S. Mohamed, M. Z. Mohamed, and M. M. Khowdairy, J. Canc. Res. Ther. **3** (2007) 198.
48. A. A. El-Awady, B. A. Abd-El-Nabey, and S. G. Aziz, J. Electrochem. Soc. **139** (1992) 2149.
49. H. M. Abd El-Lateef, V. M. Abbasov, L. I. Aliyeva, E. E. Qasimov, I. T. Ismayilov, and M. M. Khalaf, Egypt. J. Pet. **22** (2013) 451.
50. H. M. Abd El-Lateef, A. M. Abu-Dief, and B. E. M. El-Gendy, J. Electroanal. Chem. **758** (2015) 135.
51. A. S. El-Tabei, M. A. Hegazy, A. H. Bedair, and M. A. Sadeq, J. Surfact. Deterg. **17** (2014) 341.
52. O.Olivares, N. V. Likhanova, B. Gomez, J. Navarrete, M. E. Llanos-Serrano, E. Arce, and J. M. Hallen, Appl. Surf. Sci. **252** (2006) 2894.

53. E. E. Ebenso, I. B. Obot, and L. C. Murulana, Int. J. Electrochem. Sci. **5** (2010) 1574.
54. Z. Szklarska-Smialowska and J. Mankowski, Corros. Sci. **18** (1978) 953.
55. S. A. Refay, F. Taha, and A. M. Abd El-Malak, Appl. Surf. Sci. **236** (2004) 175.
56. F. Bentiss, M. Lebrini, and M. Lagrenée, Corros. Sci. **47** (2005) 2915.
57. X. Li, S. Deng, and H. Fu, Corros. Sci. **53** (2011) 302.
58. E. A. Noor and A. H. Al-Moubaraki, Mater. Chem. Phys. **110** (2008) 145.
59. E. Kraka and D. Cremer, J. Am. Chem. Soc. **122** (2000) 8245.
60. A. Vektariene, G. Vektaris, and J. Svoboda, ARKIVOC **7** (2009) 311.
61. A. M. Al-Sabagh, N.Gh. Kandil, O. Ramadan, N. M. Amer, R. Mansour, and E. A. Khamis, Egypt. J. Pet. **20** (2011) 47.
62. B. Xu, W. Yang, Y. Liu, X. Yin, W. Gong, and Y. Chen, Corros. Sci. **78** (2014) 260.
63. R. G. Parr, L. Szentpaly, and S. J. Liu, Am. Chem. Soc. **121** (1999) 1922.
64. A. Nataraj, V. Balachandran, and T. Karthick, J. Mol. Struct. **1031** (2013) 221.
65. M. Mahdavian and S. Ashhari, Electrochim. Acta **55** (2010) 1720.

Supplementary material: The online version of this article (DOI: 10.1515/zpch-2015-0616) provides supplementary material for authorized users.